



The development of the crystalline lens is sensitive to visual input in the African cichlid fish, *Haplochromis burtoni*

Ronald H.H. Kröger^{a,b,*}, Melanie C.W. Campbell^c, Russell D. Fernald^d

^a Institute of Neuroscience, University of Oregon, Eugene, OR 97403, USA

^b Institute of Anatomy, Eberhard-Karls University, Tübingen, Germany

^c School of Optometry, University of Waterloo, Waterloo, Ont., Canada N2L 3G1

^d Program in Neuroscience and Department of Psychology, Stanford University, Stanford, CA 94305, USA

Received 12 October 1999; received in revised form 11 July 2000

Abstract

We investigated whether the development of the vertebrate crystalline lens is sensitive to visual input. The optical properties of fish lenses were examined as a function of lens size and the optical rearing conditions. Fish (*Haplochromis burtoni*, Cichlidae) were reared in white light (control group), under spectral deprivation (monochromatic lights), deprivation of the cone system (scotopic illumination), and complete visual deprivation (darkness). Longitudinal spherical aberrations (LSAs) and refractive index profiles of the lenses were measured with thin laser beams. The performance of the lens was modeled by ray-tracing calculations from measured LSAs. In lenses from the control group, LSA and f/R (focal length relative to lens radius) decreased as a function of age. The optical properties of the lenses were modified after rearing in darkness, scotopic illumination, and in monochromatic lights due to changes in the refractive index profile. Rearing in darkness and scotopic illumination reduced the optical quality of the lens. In animals reared under spectral deprivation, the lens did not create well-focused images for all spectral cone types in the same plane, as it does in animals reared in white light. We conclude that visual input seems to play an important role in the development of the lens. The control mechanisms remain unknown © 2001 Elsevier Science Ltd. All rights reserved.

Keywords: Fish; Crystalline lens; Physiological optics; Refractive index gradient; Spherical aberration; Development

1. Introduction

Refractive state of the vertebrate eye can be influenced by the visual environment during development. Effects on the growth of the ocular globe and/or on the curvature of the cornea have been demonstrated in a variety of species (e.g. Sherman & Norton, 1977; Wiesel & Raviola, 1977; Wallman, Turkel, & Trachtman, 1978; Wiesel and Raviola, 1979; Gollender, Thorn, & Erickson, 1979; Kirby, Sutton, & Weiss, 1982; Nathan, Crewther, Crewther, & Kiely, 1984; Gottlieb, Fugate-Wentzek, & Wallman, 1987; Wallman, Gottlieb, Rajaram, & Fugate-Wentzek, 1987; Schaeffel, Glasser, & Howland, 1988; Schaeffel, Troilo, Wallman, & Howland, 1990; Irving, Sivak, & Callender, 1992; Kröger &

Wagner, 1996). Results obtained from the chick eye suggest that during emmetropization, i.e. the fine-tuning of the refractive state of the eye towards emmetropia, the average power of the crystalline lens is constant while eye size and the spacings of the optical elements of the eye are adjusted to the visual needs of the animal (Schaeffel & Howland, 1988; Sivak, Ryall, Weerheim, & Campbell, 1989). Here we investigated changes in the fish crystalline lens with age and rearing condition, and whether changes in the lens could also produce changes in the optical function of the eye.

Vertebrate crystalline lenses have an internal gradient of refractive index which reduces aberrations, most notably spherical aberration, and increases the mean refractive power of the lens (Campbell & Hughes, 1981). This gradient achieves its maximum in the eyes of fishes where the lens is spherical. The focusing ability of the typical fish eye almost exclusively resides in the lens, since the contribution of the cornea is negligible in

* Corresponding author. Present address: Department of Zoology, University of Lund, Helgonavägen 3, 223 62 Lund, Sweden.

E-mail address: ronald.kroger@zool.lu.se (R.H.H. Kröger).

water due to the similarity in refractive index (Matthiessen, 1886). Additionally, focal length relative to lens size is short, usually in the range of 2.2–2.8 lens radii (Fernald, 1988). The refractive index profile of the lens therefore is steep to achieve such high refractive power. Due to a small f -number (focal length divided by the diameter of the aperture) the defocusing effect of the longitudinal chromatic aberration (LCA) by far exceeds the depth of field of the fish eye. To make color vision with reasonable spatial resolution possible, fish lenses have longitudinal spherical aberrations (LSA) which produce caustics (regions near the focal point of the lens) of complex shapes which lead to multiple focal points in monochromatic light. Because of LCA, each of these focal points coincides with the retinal plane at a different wavelength. The spacings between the focal points are such that in full-spectrum illumination there is a well-focused image for each spectral cone type (Kröger, Campbell, Fernald, & Wagner, 1999a). The tuning of the focal lengths to the species-specific complement of spectral classes of cone necessitates exact control over the refractive index profile. Fishes are therefore well suited for the study of mechanisms that control the optical development of the crystalline lens, since small changes in the refractive index profile have large effects on image quality.

Haplochromis burtoni from Lake Tanganyika (Fernald & Hirata, 1977) was chosen for this study since the species critically depends on color vision for social interactions and other tasks (Fernald, 1977, 1984). Conspicuous body color patterns, which serve as important social signals, correlate with a sophisticated, trichromatic visual system (Fernald & Liebman, 1980; Fernald, 1981; Allen & Fernald, 1985). Furthermore, the optical properties of the radially symmetrical lenses of *H. burtoni* reared in white light regimes have been investigated in detail (Fernald & Wright, 1985; Kröger, Campbell, Munger, & Fernald, 1994; Kröger & Campbell, 1996; Kröger et al., 1999a).

We measured refractive index profiles and LSAs in two, partially overlapping sets of lenses. First, we studied lenses of different sizes to investigate the effects of lens growth in animals reared under white light. Second, fish were reared in constant darkness, scotopic illumination, three monochromatic lights, and in white light to address the question of whether the development of the lens is sensitive to visual input.

2. Materials and methods

2.1. Animals

The animals used in this study were bred from a laboratory population drawn from a large and diverse founder population (Fernald & Hirata, 1977). Inbreed-

ing has been largely avoided since then. All fish were kept at 27°C, pH 8.0–8.5. The age range was from the age of sexual maturity (approx. 3 months) to about 3 years of age, which is approx. half the maximum lifespan of *H. burtoni*. Age related deterioration of lens quality can therefore be excluded. One set of aquaria was illuminated with full spectrum fluorescent tubes (Spectralite). Light intensity was two to three orders of magnitude above photopic threshold (Fig. 1). These fish were used to study the effects of growth on the refractive properties of the lens.

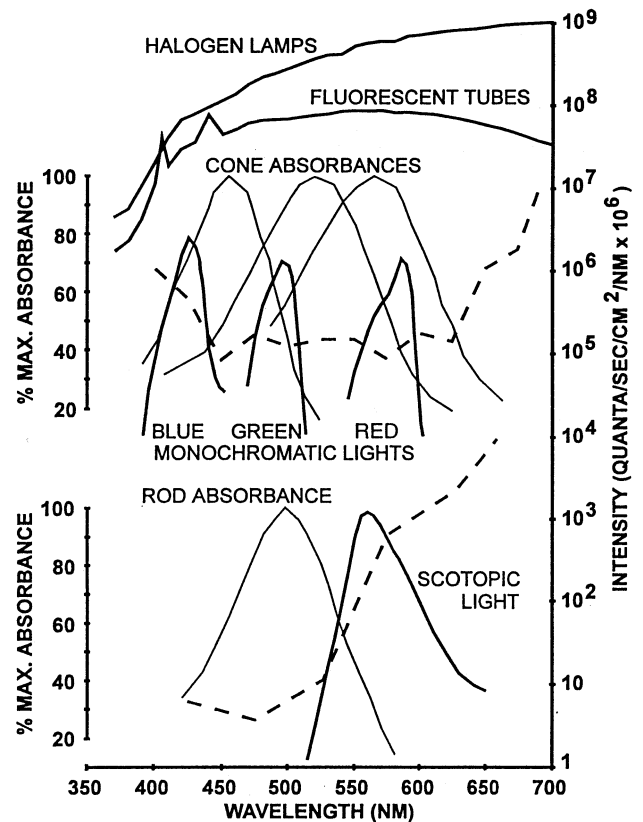


Fig. 1. The absorption spectra of the three cone types of *H. burtoni* (left vertical axes, thin lines) and the spectral light intensity distributions in the aquaria (right vertical axis, bold lines). Broken lines indicate threshold stimulus irradiances for photopic and scotopic vision. Upper curves: the spectral location of the 'green' light was chosen such that it fell between the absorption spectra of the short-wave and long-wave sensitive cones, giving about 80% of the maximum stimulation to the middle-wave sensitive cones. The other two monochromatic lights were chosen to give about the same amount of stimulation to the short-wave and the long-wave sensitive cones as the middle-wave sensitive cones received by the 'green' light. The upper two spectra were measured for halogen light filtered through 10 cm of water and for full spectrum fluorescent tubes (Spectralite). Lower curves: due to low-power operation of the green light-emitting diodes used for scotopic illumination, their spectrum was somewhat red-shifted and did not match the peak absorbance of the rods very well. The maximum difference between scotopic threshold and light intensity could nevertheless be adjusted to about one order of magnitude, while keeping maximum intensity about two orders of magnitude below photopic threshold.

For the study of effects of the lighting condition, additional aquaria were placed in light-tight boxes which allowed the stringent control of the light environment. At day 3 after fertilization (Hagedorn & Fernald, 1992) eggs were taken from the mouth-brooding females and placed under the chosen lighting conditions. At this stage the eye is still entirely transparent with no pigments present. The embryos were artificially incubated for about 10 more days until the young animals were able to swim on their own. The fish were maintained for about 10 months before measurements were performed. All fish in illuminated aquaria were in a 12 h–12 h light–dark cycle. There were seven different rearing groups:

Control group. Fish were maintained in aquaria illuminated with the broad spectrum light of halogen lamps. A 10 cm water filter was used to remove infrared and ultraviolet radiation. Light intensity in mid-water of the aquarium was three to four orders of magnitude above photopic threshold (Fig. 1). Additional fish of the same age were maintained under full spectrum fluorescence light (Spectralite). Since there were no detectable differences between these sub-groups, the data were pooled in the analysis to constitute a large white light control group ('white'). *Monochromatic light groups* ('blue', 'green', 'red'). Three groups of fish were kept in aquaria illuminated with lights of narrow spectral bands produced with 10 nm bandwidth interference filters in combination with halogen lamps. The transmissions of the interference filters were matched to the absorbances of the cone photoreceptor pigments such that in each group one type of cone received about the same amount of stimulation as the other cones in the other groups, with as little overlap as possible. Light intensities were approximately the same in all three boxes and about one order of magnitude above photopic threshold (Fig. 1).

Scotopic illumination group ('dim'). This group of fish was kept in very dim light produced by light emitting diodes placed in the roof of one box about 45 cm above the water surface in the aquarium. Light intensity was adjusted to one order of magnitude above scotopic threshold, which is at least two orders of magnitude below photopic threshold (Fig. 1).

Darkness group ('dark'). One group of fish was reared in an aquarium in a light-tight box with no light source.

The inside of the box housing the darkness group was painted flat black. The insides of all other boxes were painted flat white. Light distribution across the aquaria was made as even as possible by diffusors in front of the light sources. For further details on the rearing conditions and light intensity measurements see (Kröger & Fernald, 1994).

2.2. Measurements

Fish were transported from the Institute of Neuroscience (Eugene, OR, USA) to the School of Optometry (Waterloo, Ont., Canada) where the measurement apparatus and image processing system used in this study were located, and kept there in the light of full spectrum fluorescent tubes. Measurements were begun the day after arrival and were completed within 3 weeks. Only fish that appeared healthy by visual inspection were used. One fish at a time was sacrificed by rapid decapitation and the lens of one eye was immediately excised to determine either its refractive index profile or its spherical aberration. The second lens was excised about 1–2 h later and treated in the same way as the first lens.

To measure the refractive index profile, thin, parallel beams of red laser light (HeNe, $\lambda = 633$ nm) were shone through a meridional plane of the lens, which was suspended in a solution of saline and polyvinylpyrrolidone (Campbell, 1984). The refractive index of this solution (1.361 at 633 nm) matched the surface index of the lens (Kröger et al., 1994). We assumed, for reasons given in the discussion, that the refractive index of the surface of the lens is independent of lens size and light regime during development. Lens shape and the paths of 70–100 beams before and after deflection by the lens were recorded with an image capturing and processing system. Since the lens of *H. burtoni* is spherical with a radially symmetrical distribution of refractive index (Kröger et al., 1994), the refractive index profile can be calculated from the entrance positions y , i.e. the lateral distances between the optical axis and the entrance beams, and the angular differences between entrance and exit beams $F(y)$ (Chu, 1977; Campbell 1984). Since the analysis of the deflection data includes a numerical integration (Chu, 1977; Campbell, 1984; Kröger et al., 1994) discrete data points for $F(y)$ had to be transformed into a continuous deflection function. We used linear interpolation between data points for that purpose. One hundred data points were calculated for each refractive index profile and the 101st data point was given by the surface index of the lens. If the refractive index (n) as a function of radial position in the lens (r) was expressed in percent lens radius, the data points for $n(r)$ were equally spaced in all refractive index profiles (Kröger et al., 1994), such that $n(r_i)$ could be compared between lenses, with $1 \leq i \leq 101$.

To measure the spherical aberration, the lens was suspended in 0.9% saline ($n = 1.334$ at 633 nm). Lens size and the paths of the beams before and after deflection by the lens were recorded with the same image capturing system as for measurements of the refractive index distribution. Back vertex distances (BVDs) of the exit beams, i.e. the distance between the

posterior vertex of the lens and the crossing of the optical axis by the measured beam, were determined as a function of beam entrance position [BVD(y)]. Before further analysis, the two halves of each lens were averaged by using linear interpolation between data points. Averaging the two halves of a lens removes artificial asymmetry in the spherical aberration that stems from measurement error in the position of the axis of symmetry (Campbell, 1982). Interpolation allowed the calculation of the BVDs for beam entrance positions evenly spaced by 1% lens radius in all lenses. All BVD values were plotted as a function of normalized lens radius R (from 0 to 1). This is a measure of longitudinal spherical aberration (LSA).

Both immersion media were adjusted to an osmolarity of 290–305 mosmol, pH 7.0–7.5, and were used at room temperature. The measurement system and the methods of data analysis for both types of measurements are described in more detail elsewhere (Campbell, 1984; Kröger et al., 1994).

2.3. Ray-tracing model calculations

To model the performance of fish lenses, we used a two-dimensional ray-tracing model (Kröger et al., 1994). The lens was represented in the model as a structure with concentric, iso-indicial layers. Refraction of a ray of light was calculated from layer to layer using Snell's law. The ray-tracing program interpolated between the 101 data points of a refractive index profile using a cubic spline and assigned refractive indices to 30,000 layers to simulate a locally smooth gradient. In order to increase accuracy in the periphery of the lens where the gradient of refractive index is steep, the spacings between layers followed a parabolic function such that many thin layers were placed into the periphery.

The paths of beams deflected by the lens were known from the measurements of LSA and independently from model calculations. The distribution of light on planes at different distances from the lens could thus be determined by simple geometric ray-tracing (Kröger et al., 1999a). The effective aperture of the fish lens was set to 1.9 lens radii (R) since most of the energy of rays with entry position larger than $0.95R$ is reflected (Sroczyński, 1976). Focal length of the *H. burtoni* lens is about $2.3R$ at 633 nm (Kröger et al., 1994). The diameter of the Airy disc in diffraction limited optics would thus be $0.001R$ at 350 nm and $0.002R$ at 700 nm. The sampling interval in an image plane was set to an intermediate value ($0.0015R$) in all calculations.

3. Results and analysis

To determine the sources of variability, we averaged

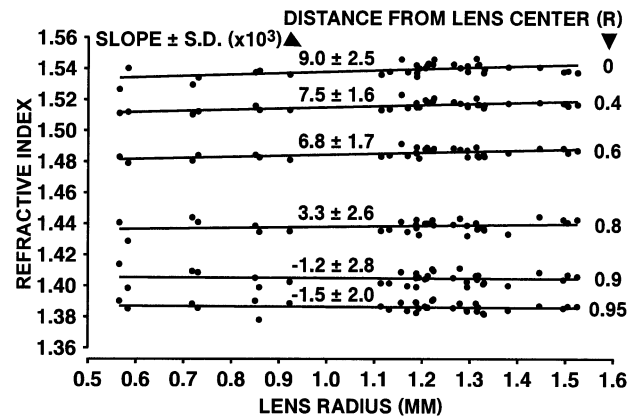


Fig. 2. The relationship between lens size and refractive indices in the *H. burtoni* lens. Refractive index in the same relative position increases with increasing lens size. 100 lines of regression (only six are shown) were fitted to the data and used to interpolate refractive index profiles for lenses of any chosen size within the size range of the studied lenses. Note the increase of refractive indices with increasing lens size in the central regions of the lenses. The slope numbers represent the slopes multiplied by 10^3 .

the variances of the measured LSAs and refractive index profiles across lens radius. From those values, we calculated the mean inter-animal variances (after averaging the results from both lenses of each fish) and mean intra-animal variances (between both lenses of each fish). In the animals of similar sizes used to determine the effects of the visual environment, the inter-animal variances were smaller than the intra-animal variances (e.g. 'white' group: LSA: inter = 0.0032, intra = 0.0049; refractive index profile: inter = 4.6×10^{-6} , intra = 1.1×10^{-5}). This indicates that measurement uncertainties rather than inter-individual differences were the main source of variation. All data were therefore treated as independent measurements.

3.1. Effects of growth

A total of 35 refractive index profiles were determined for the lenses of 21 fish reared in white light. Lens radius ranged from 0.566 to 1.525 mm. Larger lenses had higher refractive index in the central region (Fig. 2). Refractive index at the i th measurement positions in the lenses can be well described as linear functions of lens size (Fig. 2). Therefore, linear regression was used to describe the change in refractive index at corresponding normalized radial positions, r_i , as a function of lens size in the form of

$$n(r_i, R) = Rm_i + b_i \quad (1)$$

where R is the lens radius, m_i is the slope, and b_i is the intercept of the i th line of regression. The slopes of the lines of regression were significantly ($p < 0.05$, ANOVA) higher than zero between 0 and $0.62R$, and

Table 1
Lenses of similar sizes were selected to study the effects of the different lighting conditions during development on the refractive index profile and the spherical aberration of the *H. burtoni* lens

Type of illumination	Type of measurement		Spherical aberration	
	Refractive index profile		Average lens radius (mm)	
	Average lens radius (mm)	<i>N</i>	Average lens radius (mm)	<i>n</i>
'White'	1.228 ± 0.153	20	1.104 ± 0.120	21
'Blue'	1.237 ± 0.045	8	1.241 ± 0.011	6
'Green'	1.240 ± 0.044	8	1.171 ± 0.077	6
'Red'	1.237 ± 0.025	8	1.272 ± 0.055	6
Scotopic illumination	1.142 ± 0.082	6	1.162 ± 0.106	6
Darkness	1.077 ± 0.036	12	1.097 ± 0.021	8

not significantly different from zero in the periphery of the lens.

The measured refractive index profiles of all lenses can be converted to that of a lens of any radius X within the range of the radii of the lenses used in this study with

$$n(r_i, X) = n(r_i, R)_{\text{measured}} + m_i(X - R) \quad (2)$$

When all measured refractive indices from fish reared in white light were converted with Eq. (2) using $X = 1.2$ mm, which is about the mean radius of all lenses used in this part of the study (Table 1), those size-corrected refractive indices showed less variation than the raw data (Fig. 3), indicating that some of the variance was due to size-related differences.

By using the linear regressions for the relationship between lens size and the refractive index at corresponding positions in the lenses, a representative refractive index profile could be interpolated for a lens of any chosen size within the range of lens sizes investigated in this study. Interpolated profiles are more accurate than individual, measured profiles since they are based on a larger number of measurements. With Eq. (1) we determined representative refractive index profiles for the largest and the smallest lens in our sample. As expected from Fig. 2, the resulting profiles were very similar between 100% and about 85% lens radius, but then diverged centralward (see inset in Fig. 3). The central index in the smallest lens was about 0.008 lower than in the largest lens. Slight depressions in the refractive index profiles were present at the same relative radial position irrespective of lens size (arrowheads in Fig. 3). In lenses of animals reared in white light, these depressions are correlated with structure in the LSA curve (Kröger et al., 1994)

The optical consequences of size-related differences in the refractive index profiles were studied in a ray-tracing simulation. The LSA of larger lenses is smoother and relative focal length is shorter (Fig. 4). However, LSA of complex shape was present in all

lenses. Although there is close agreement between modeled and measured LSA (Kröger et al., 1994), it was not possible to predict LSAs in such detail that the multiple focal lengths of the lenses became as evident as from measured LSAs.

In additional sets of ray-tracing simulations we addressed the question of whether the observed difference in f/R between small and large lenses could be due to a change in surface index rather than differences in central indices. Two possible scenarios of differences between small and large lenses were investigated, using 100 rays in each calculation. First, the central index

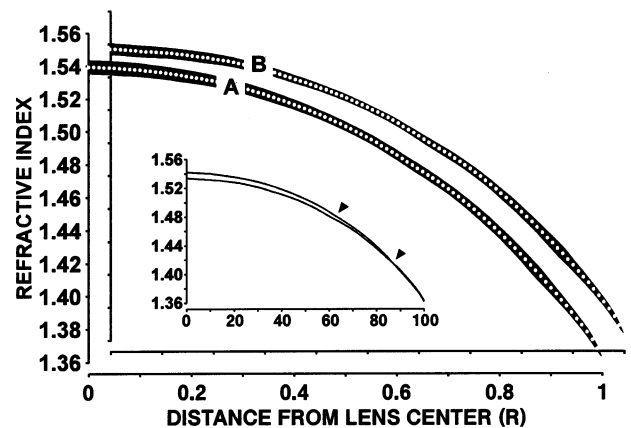


Fig. 3. Refractive index in the *H. burtoni* lens decreases from the center to the surface of the lens from about 1.54 to 1.361. The black area is the range of standard deviations, dots mark the mean refractive indices. Curve (A) shows the averaged raw data, while curve (B) shows the average refractive index profile after all profiles from fish reared in white light had been converted to a lens radius of 1.2 mm with Eq. (2). The spread in the latter data is reduced in comparison with the raw data (average SD 0.0023 vs. 0.0029), indicating that at least some of the variation in refractive indices related to lens size has been removed. The inset shows refractive index profiles which were interpolated by using Eq. (1) for the largest and the smallest lens in the size range of the lenses of fish reared in white light. Note that refractive indices are higher in the central region of the larger lens. The central indices differ by about 0.008. Slight depressions in the refractive index profiles (arrowheads) are at about the same relative radial locations irrespective of lens size.

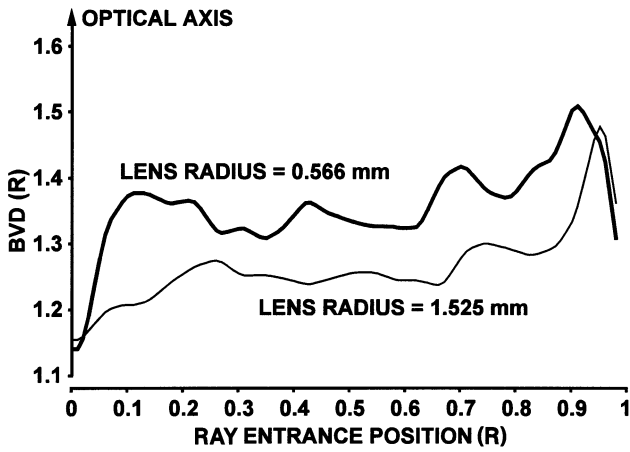


Fig. 4. Spherical aberration curves (back vertex distances, BVD, normalized to lens radius R , vs. normalized ray entrance position) calculated from the refractive index profiles as shown in the inset of Fig. 3 for the largest and the smallest lens. Since spherical aberration is symmetrical to the optical axis, only one side is shown. Relative focal length is shorter in the larger lens. Furthermore, there is structure in the spherical aberration curves irrespective of lens size.

remained unchanged while more peripheral indices were increased or decreased by linearly shrinking or stretching, respectively, the index profile along the n -axis. Second, all indices were increased or decreased by the same amount. The refractive index profile of a medium sized reference lens of 1.2 mm radius was modified such that the surface index was 0.01 higher or lower than the measured surface index of 1.361 (Fig. 5A). With the modified profiles, a first set of model calculations was performed with the lens immersed in a medium of $n = 1.334$ to study the effects on focal length and on spherical aberration. In a second set of model calculations, the index of the surrounding medium was set to 1.361 to simulate measurements of refractive index profiles with index mismatches between the lens surface and the immersion medium. The modeled ray paths were analyzed like measured beam paths to determine whether measurements of central indices are affected by an index mismatch at the lens surface. In a third set of model calculations the refractive index profiles recalculated from the simulated measurements were used to model spherical aberrations as they would be predicted from measurements of refractive index profiles with lens surface indices that are higher or lower than the index of the immersion medium.

Introducing a difference in surface index of 0.02 (Fig. 5A) produced a shift of about $0.01R$ in paraxial focal length as well as in BVDs of rays with entrance positions of up to about $0.6R$. For more peripheral beam entrance positions, the differences in BVDs were more dramatic (Fig. 5B). The results of the model calculations also show that a moderate mismatch in refractive index between the lens surface and the immersion medium influences refractive index measurements (Fig.

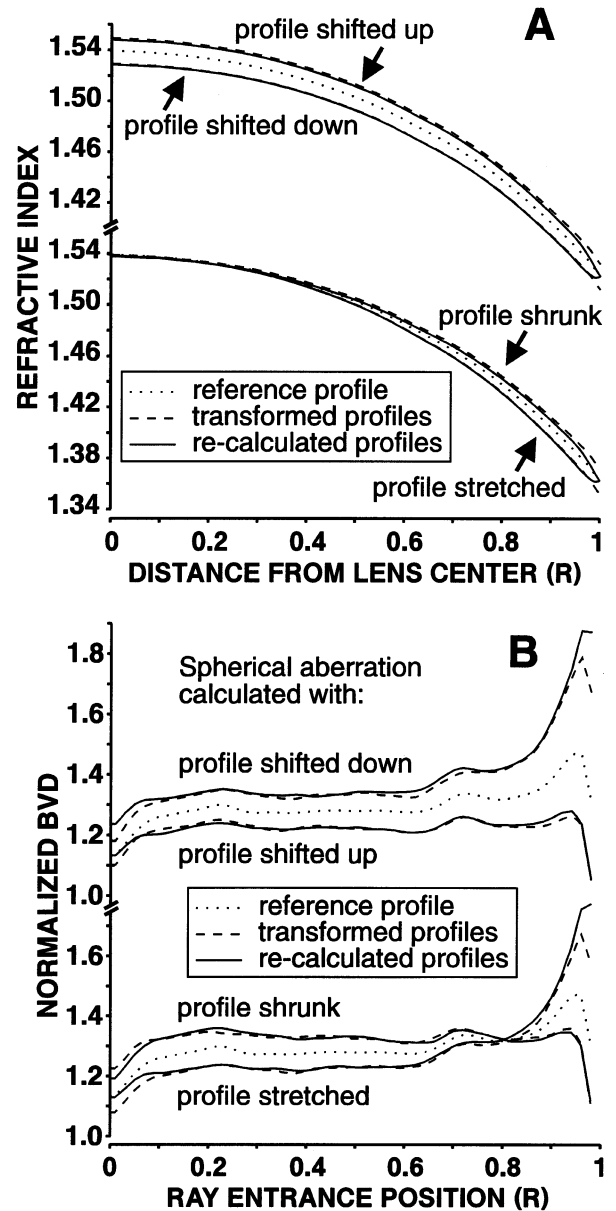


Fig. 5. The profile of a reference lens of 1.2 mm radius (A, stippled line) was modified by linear stretching or shrinking along the refractive index axis and by shifting it up or down (A, dashed lines). Calculated spherical aberrations with the surrounding index set to 1.334 show that a difference in surface index of 0.02 induces differences in BVDs of about $0.01R$ over most of the aperture (B, dashed lines), similar to the differences in focal length observed between small and large lenses. Near the edge of the lens, however, the curves have different inclinations, which is unlike the differences between the modeled spherical aberrations of small and large lenses (compare with Fig. 4). If measurements of refractive index profiles are simulated by setting the surrounding index to 1.361, refractive index profiles recalculated from modeled ray paths are very similar to the original, modified profiles (A, continuous lines). Notable differences in refractive index are restricted to the periphery of the lens, in contrast to the observed differences between small and large lenses (compare with Fig. 3). Differences between spherical aberrations calculated from the modified (B, dashed lines) and from the recalculated profiles (B, continuous lines) are also small, indicating that the method is robust to moderate errors in surface index.

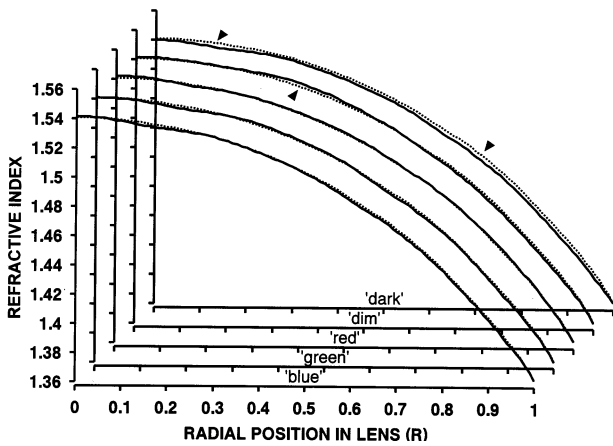


Fig. 6. Refractive index profiles of lenses of fish reared in the various light regimes (Fig. 1) have been converted to a lens radius of 1.2 mm (Eq. (2)) and averaged (solid lines). They are compared with the reference profile of a lens of 1.2 mm radius (dotted lines) that was interpolated from the data of the 'white' group (Fig. 2, Eq. (1)). The refractive index profiles of the darkness ('dark') and scotopic illumination ('dim') groups differ visibly (arrowheads) from the reference profile. Although the refractive index profiles of the lenses of fish reared in monochromatic lights ('blue', 'green', 'red') seem to be similar to the reference profile, statistically significant differences were present in the 'blue' and 'green' groups (Fig. 7).

5A) and predictions of spherical aberrations (Fig. 5B) much less than one might expect. Notable differences between the original and the recalculated spherical aberration were restricted to the periphery of the lenses. Differences in the surface index therefore cannot explain the differences in refractive index observed deep within the lenses.

3.2. Effects of lighting conditions

To minimize possible masking effects of differences due to lens size, we selected fish of similar sizes for the study of the influence of lighting conditions on the refractive index profiles. From the white light group, only those lenses were included that came from fish of the same age as the fish in the other light regimes. This sub-sample of 20 lenses from 10 fish did not include very small and very large lenses (Table 1). Differences due to the remaining variation in lens size were at least partially eliminated by using Eq. (2) to convert all profiles to a lens radius of 1.2 mm.

At first sight, the mean refractive index profiles in the monochromatic light groups are similar to the white light reference profile (Fig. 6). However, the profiles obtained from the 'green' and 'blue' groups were significantly different ($P < 0.05$) from the white light reference profile at about $0.18R$ (Fig. 7A). The mean profiles in the 'dim' and 'dark' groups differed even more from the reference profile (Figs. 6 and 7B). The lenses in the 'dark' group were not similar to young lenses from the 'white' group, since lenses of similar sizes from both

groups had about the same central index and different indices in the periphery (Fig. 6), a region where small and large lenses of the control group had similar indices (Fig. 3).

Spherical aberrations were measured in 16 lenses from eight fish in the white light control group. To increase the size of this group, we included the data of five lenses from five fish in the same size range from an earlier study (Kröger et al., 1994) such that the white light control group comprised 21 lenses from 13 ani-

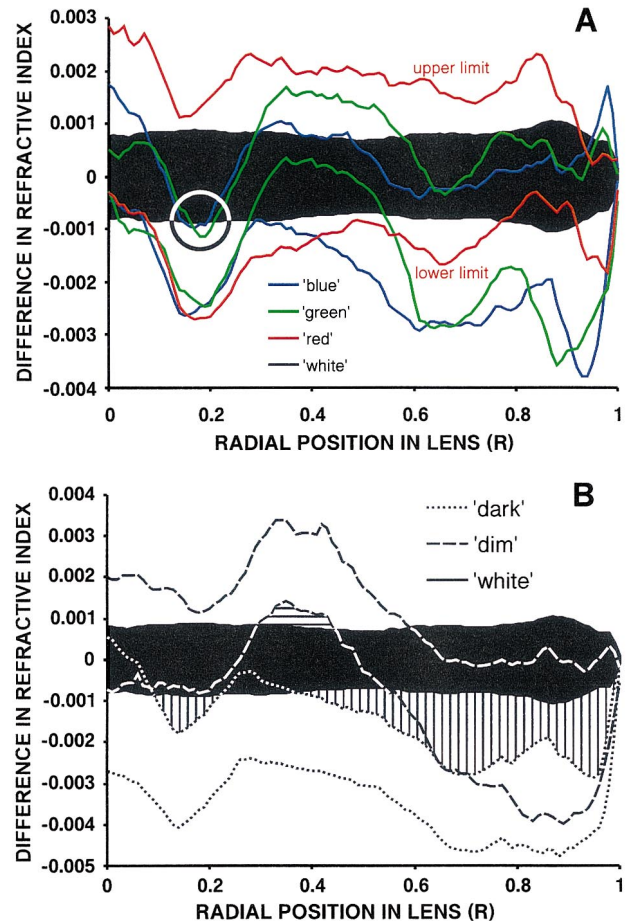


Fig. 7. To demonstrate the differences in the refractive index profiles, all measured profiles were converted to a lens radius of 1.2 mm with Eq. (2). Thereafter, the reference profile for a lens of the same radius ('white' group) was subtracted from all profiles to make the differences in refractive index independent of the absolute indices. Finally, the 90% confidence intervals for the differences from the reference profile were calculated and plotted for all rearing groups. Where two confidence intervals do not overlap, the profiles are statistically different on the $p < 0.05$ level. The confidence interval of the 'white' group is plotted as the black area, the borders of the other intervals are displayed as color-coded lines. (A) The profiles from the 'blue' and 'green' groups had statistically lower indices than the profiles in the 'white' group at about $0.2R$ (circle). (B) The refractive index in the darkness group was significantly lower than in the profiles from the 'white' group almost along the entire lens radius (vertically shaded area). In the scotopic illumination group, the refractive index was significantly higher in the region around $0.4R$ (horizontally shaded area).

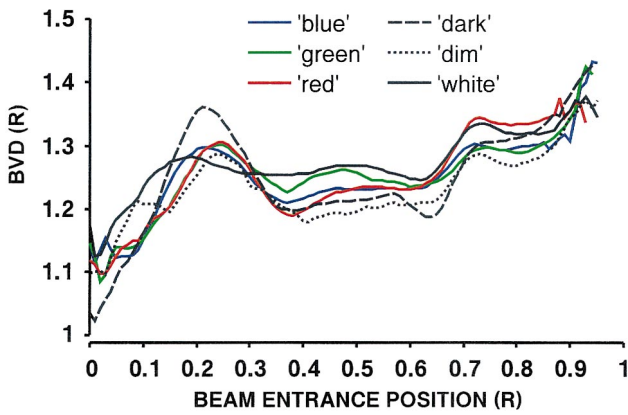


Fig. 8. Mean measured longitudinal spherical aberrations (LSAs) in a color-coded plot. The LSAs of animals reared under visual deprivation conditions are different in shape from the LSA of the 'white' group. These data were used to determine the focusing properties of the lenses (Fig. 9).

mals. Variances in the measured LSAs were higher than in the refractive index profiles, since the former measurements are sensitive to disturbances of the lens surface. The differences between the LSAs obtained from the various rearing groups (Fig. 8) were therefore not statistically significant. However, there were obvious optical differences: the focal lengths were poorly defined in the 'dim' and 'dark' groups (Fig. 9). In the 'blue' and 'red' groups, the lenses were bifocal. In the 'green' group, the spacings between the focal lengths did not match the differences in focal length due to LCA between the wavelengths of maximum cone absorbance (Fig. 9).

4. Discussion

Our results indicate that the quality and relative focal length of the lens change during growth and that visual

Fig. 9. Levels of retinal irradiance (monochromatic light) within a circular area around the optical axis of a radius of $0.0015R$ were derived from the averaged LSAs shown in Fig. 8 as a function of the axial distance from the lens. Three well-defined peaks in the 'white' group mark the typical three, axially separated foci of the *H. burtoni* lens (Kröger et al., 1999a). Black dots mark the axial locations of the foci predicted for optimal compensation of longitudinal chromatic aberration (Kröger & Campbell, 1996). With the retina at the location indicated by the vertical stippled line (top graph), middle-wave (green) light is focused on the retina by the middle focal point of the lens. For long-wave (red) light, the refractive power of the lens is somewhat lower and the anterior focal point is shifted away from the lens to the axial position of the retina. The power of the lens is considerably higher for short-wave (blue) light, which is focused on the retina by the posterior focal point of the lens. In the 'dim' and 'dark' groups, the foci were shifted axially relative to the lens and to each other, and were poorly defined. The animals in the 'blue' and 'red' groups had bifocal lenses. In the 'green' group, the spacings between the three foci were not suitable for good compensation of longitudinal chromatic aberration.

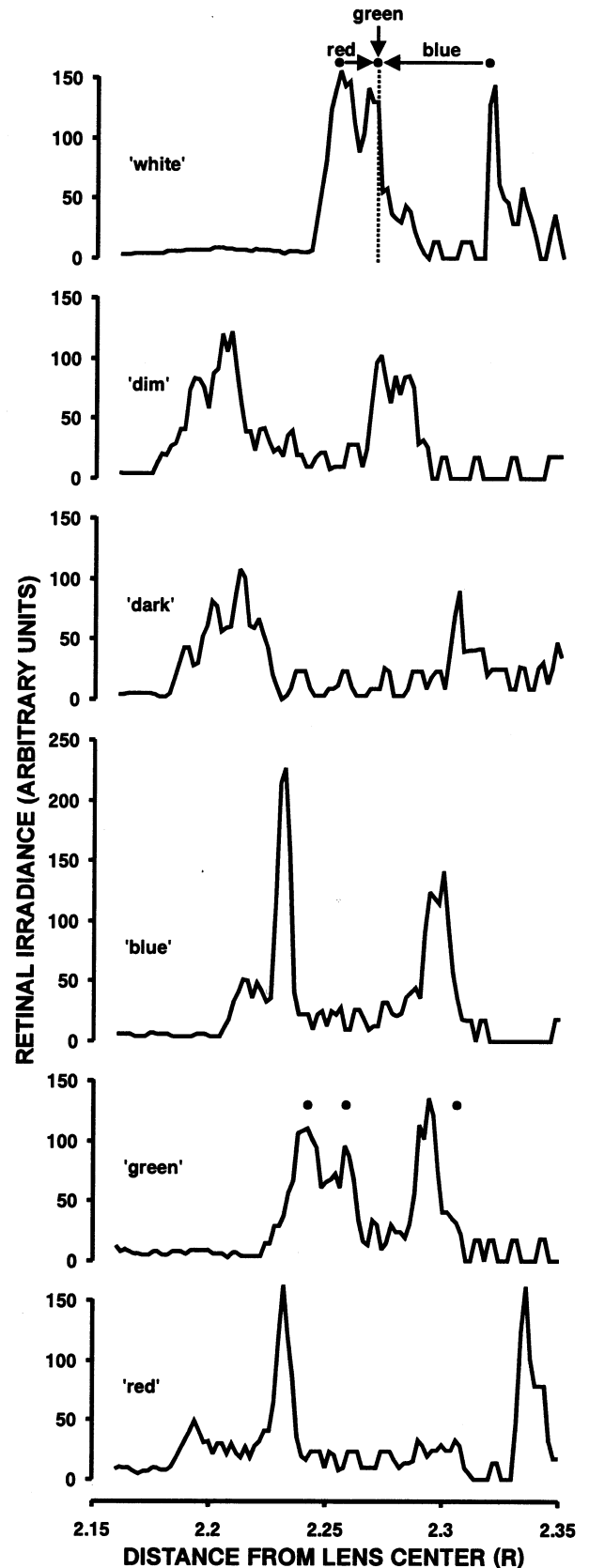


Fig. 9.

deprivation appears to disrupt the tuning between the multiple focal lengths and the absorbances of the spectral cone types, which is necessary to compensate for the defocusing effect of LCA (Kröger et al., 1999a). The optical properties of the fish lens therefore appear to be fine-tuned during development by visual input. A closed-loop feedback system may be involved. Precise control of the refractive index gradient is also suggested by the fact that the small indentations in the profile remain in the same relative radial positions during growth of the lens (Fig. 3). Those deviations from a smooth profile move outward in step with lens growth. Therefore, they cannot be due to the properties of individual lens fiber cells, which cannot change position in relation to neighboring cells. This suggests a specific function rather than a defect. We presume that the indentations mark the borders between the zones of different focal lengths.

Although the differences in the profiles obtained from the different rearing groups were small, the consequences for lens performance were severe, as is illustrated by the ray-tracing calculations based on the measured LSAs (Fig. 9). For appropriate lens function, the refractive index profile therefore has to be adjusted with great accuracy. It is an interesting question how such accuracy can be achieved during constant growth, in particular as the bulk of the lens fiber cells is 'dead', i.e. they have lost all organelles including the nucleus. Despite the inability of individual fiber cells to synthesize proteins and to generate energy, the refractive index gradient is correctly maintained during growth of the lens. Furthermore, the index profile does not simply scale as a function of lens size but changes slightly to give improving image quality as the lens grows.

Substances and signals can be exchanged within the lens via gap-junctions and possibly other pathways of cell-to-cell communication (Bassnett, Kuszak, Reinisch, Brown, & Beebe, 1994; Kuszak, Novak, & Brown, 1995; Rae, Bartling, Rae, & Mathias, 1996). It is unknown, however, how or whether signals from the retina and/or the brain reach the lens. Such signals in turn could influence the quality of the image. There is evidence that neuroactive substances released in the retina influence the optics of the lens. If the dopaminergic system of the fish retina is selectively destroyed, which depletes the eye of diffusing dopamine, the focal length of the lens decreases (Kröger, Hirt, & Wagner, 1999b). It is therefore conceivable that signalling substances released in the retina act on the optical properties of the lens, which is reached by diffusion. How or if such compounds take effect in the lens and how image quality is determined are questions which remain unanswered to date.

To compensate for LCA, the lenses of the white light group are multifocal, producing a relatively sharp im-

age on the retina for each of the cone types in white light (Kröger et al., 1999a). In monochromatic light, a monofocal lens with good correction of LSA would produce the best image for all spectral cone types, since the LCA of the lens is irrelevant under such conditions. Rather than having an ideal monofocal lens (no LSA), monochromatically reared fish appeared to lose some multifocality and become (on average) bifocal ('red' and 'blue') or trifocal ('green'). The effects on the mean focal length were minor (Fig. 9). Thus, only the fine structure of the lens appears to be sensitive to visual input.

4.1. Refractive index at the lens surface

The refractive index at the surface of the lens is difficult to measure, since the gradient of refractive index is steep in the periphery of the lens. The simulated measurements with mismatches between the surfaces index of the lens and the index of the immersion medium show that if the refractive index of the lens surface is overestimated, i.e. the index of the immersion medium is too high, the mismatch would result in a characteristic indentation in the measured profiles close to the lens surface (Fig. 5A). An index of the immersion medium that is chosen too low would be much less obvious. We do not expect notable variation of refractive index across the surface of the lens, since measured refractive index profiles were independent of the axis of measurement (Kröger et al., 1994).

The physiologically active cells in the lens periphery have to provide all necessities for the entire lens. Non-specialized cells have protein concentrations of 15–17 g per 100 ml cytoplasm and refractive indices of 1.361–1.364 (at 590 nm; Barer, 1957, which is almost identical to the values we found in the outer periphery of the fish lens (Kröger et al., 1994). It therefore seems likely that the surface index of the lens is determined by the minimum needs for protein contents of lens epithelium cells and differentiating lens fibers. We have therefore assumed that the refractive index of the surface of the lens is independent of lens size and light regime during development. Furthermore, our ray-tracing simulations show that refractive index measurements are surprisingly resistant to moderate mismatches between the immersion medium and the lens surface (Fig. 5). It is therefore unlikely that the observed changes in the refractive index profiles are due to bias caused by differences in surface index.

4.2. The control of lens growth

Large *H. burtoni* lenses have relatively shorter focal lengths than small lenses, which is in agreement with observations in pike (Sroczyński, 1975) and perch (Sroczyński, 1979) that f/R and spherical aberration

decrease with increasing size of the animal. Decreasing f/R with increasing lens size was also found in the South American cichlid fish *Aequidens portalegrensis* (Baerends, Beunema, & Vogelzang, 1960). It appears to be a general pattern that the relative focal length decreases and the optical quality of the lens increases with increasing lens size in fish of the same species. In *H. burtoni*, the decrease in f/R is due to a relatively steeper refractive index gradient in larger lenses. The reduction of spherical aberration is the result of a smoothing of the refractive index profile as the lens grows (Fig. 3). Visual feedback may be involved in this process, since uncontrolled smoothing of the profile would abolish the discrete focal lengths. Multifocal lenses are also present in mammalian eyes with small f -numbers (Kröger et al., 1999a). Furthermore, central indices and the smoothness of the refractive index profile increase in bovine lenses with increasing size (Pierscionek, 1989). Those similarities suggest that the development of the mammalian lens may be under the control of mechanisms equivalent to those present in the fish eye.

Acknowledgements

We thank Sheila Vollmer for her help in rearing the fish and Rejean Munger for helpful discussions. This study was supported by DFG grant Kr 1078/1-1 to R.H.H.K., by NIH grant EY 05051 to R.D.F., and by NSERC University Research Fellowship and Research Grant to M.C.W.C.

References

- Allen, E. A., & Fernald, R. D. (1985). Spectral sensitivity of the African cichlid fish, *Haplochromis burtoni*. *Journal of Comparative Physiology*, 157, 247–253.
- Baerends, G. P., Beunema, B. E., & Vogelzang, A. A. (1960). Über die Änderung der Sehschärfe mit dem Wachstum bei *Aequidens portalegrensis* (Hensel) (Pisces, Cichlidae). *Zoologische Jahrbücher, Physiologie*, 88, 67–78.
- Barer, R. (1957). Refractometry and interferometry of living cells. *Journal of the Optical Society of America*, 47, 545–556.
- Bassnett, S., Kuszak, J. R., Reinisch, L., Brown, H. G., & Beebe, D. C. (1994). Intercellular communication between epithelial and fiber cells of the eye lens. *Journal of Cell Science*, 107, 7998–8011.
- Campbell, M. C. W. (1982). Gradient refractive index optics and image quality in the rat eye. Thesis, Canberra: Australian National University.
- Campbell, M. C. W. (1984). Measurement of refractive index in an intact crystalline lens. *Vision Research*, 24, 409–415.
- Campbell, M. C. W., & Hughes, A. (1981). An analytic, gradient index schematic lens and eye for the rat which predicts aberrations for finite pupils. *Vision Research*, 21, 1129–1148.
- Chu, P. L. (1977). Nondestructive measurement of index profile of an optical-fibre preform. *Electronics Letters*, 13, 736–738.
- Fernald, R. D. (1977). Quantitative behavioural observations of *Haplochromis burtoni* under semi-natural conditions. *Animal Behaviour*, 25, 643–653.
- Fernald, R. D. (1981). Chromatic organization of a cichlid fish retina. *Vision Research*, 21, 1749–1753.
- Fernald, R. D. (1984). Vision and behavior in an African cichlid fish. *American Scientist*, 72, 58–65.
- Fernald, R. D. (1988). Aquatic adaptations in fish eyes. In J. Atema, R. R. Fay, A. N. Popper, & W. N. Tavolga, *Sensory biology of aquatic animals* (pp. 435–466). New York: Springer.
- Fernald, R. D., & Hirata, N. R. (1977). Field study of *Haplochromis burtoni*: habitats and co-habitants. *Environmental Biology of Fish*, 2, 299–308.
- Fernald, R. D., & Liebman, P. (1980). Visual receptor pigments in the African cichlid fish, *Haplochromis burtoni*. *Vision Research*, 20, 857–864.
- Fernald, R. D., & Wright, S. (1985). Growth of the visual system of the African cichlid fish, *Haplochromis burtoni*: optics. *Vision Research*, 25, 155–161.
- Gollender, M., Thorn, F., & Erickson, P. (1979). Development of axial ocular dimension following eyelid suture in cat. *Vision Research*, 19, 221–223.
- Gottlieb, M. D., Fugate-Wentzek, L. A., & Wallman, J. (1987). Different visual deprivations produce different ametropias and different eye shapes. *Investigative Ophthalmology and Visual Science*, 28, 1225–1235.
- Hagedorn, M., & Fernald, R. D. (1992). Retinal growth and cell addition during embryogenesis in the teleost, *Haplochromis burtoni*. *Journal of Comparative Neurology*, 321, 193–208.
- Irving, E. L., Sivak, J. G., & Callender, M. G. (1992). Refractive plasticity of the developing chick eye. *Ophthalmic and Physiological Optics*, 12, 448–456.
- Kirby, A. W., Sutton, L., & Weiss, H. (1982). Elongation of cat eye following neonatal lid suture. *Investigative Ophthalmology and Visual Science*, 22, 274–277.
- Kröger, R. H. H., Campbell, M. C. W., Munger, R., & Fernald, R. D. (1994). Refractive index distribution and spherical aberration in the crystalline lens of the African cichlid fish *Haplochromis burtoni*. *Vision Research*, 34, 1815–1822.
- Kröger, R. H. H., & Fernald, R. D. (1994). Regulation of eye growth in the African cichlid fish *Haplochromis burtoni*. *Vision Research*, 34, 1807–1814.
- Kröger, R. H. H., & Campbell, M. C. W. (1996). Dispersion and longitudinal chromatic aberration of the crystalline lens of the African cichlid fish *Haplochromis burtoni*. *Journal of the Optical Society of America A*, 13, 2341–2347.
- Kröger, R. H. H., & Wagner, H.-J. (1996). The eye of the blue acara (*Aequidens pulcher*, Cichlidae) grows to compensate for defocus due to chromatic aberration. *Journal of Comparative Physiology A*, 179, 837–842.
- Kröger, R. H. H., Campbell, M. C. W., Fernald, R. D., & Wagner, H.-J. (1999a). Multifocal lenses compensate for chromatic defocus in vertebrate eyes. *Journal of Comparative Physiology A*, 184, 361–369.
- Kröger, R. H. H., Hirt, B., & Wagner, H.-J. (1999b). Effects of retinal dopamine depletion on the growth of the fish eye. *Journal of Comparative Physiology A*, 184, 403–412.
- Kuszak, J. R., Novak, L. A., & Brown, H. G. (1995). An ultrastructural analysis of the epithelial–fiber interface (EFI) in primate lenses. *Experimental Eye Research*, 61, 579–597.
- Matthiessen, L. (1886). Über den physikalisch-optischen Bau des Auges der Cetaceen und der Fische. *Pflüger's Archiv*, 38, 521–528.
- Nathan, J., Crewther, S. B., Crewther, D. P., & Kiely, P. M. (1984). Effects of retinal image degradation on ocular growth in cats. *Investigative Ophthalmology and Visual Science*, 25, 1300–1306.

- Pierscionek, B. (1989). Growth and ageing effects on the refractive index in the equatorial plane of the bovine lens. *Vision Research*, 29, 1759–1766.
- Rae, J. L., Bartling, C., Rae, J., & Mathias, R. T. (1996). Dye transfer between cells of the lens. *Journal of Membrane Biology*, 150, 89–103.
- Schaeffel, F., Glasser, A., & Howland, H. C. (1988). Accommodation, refractive error and eye growth in chickens. *Vision Research*, 28, 639–657.
- Schaeffel, F., & Howland, H. C. (1988). Visual optics of normal and ametropic chickens. *Clinical Vision Science*, 3, 83–98.
- Schaeffel, F., Troilo, D., Wallman, J., & Howland, H. C. (1990). Developing eyes that lack accommodation grow to compensate for imposed defocus. *Visual Neuroscience*, 4, 177–183.
- Sherman, S. M., & Norton, T. T. (1977). Myopia in lid-sutured tree shrew (*Tupaia glis*). *Brain Research*, 124, 154–157.
- Sivak, J. G., Ryall, L. A., Weerheim, J., & Campbell, M. C. W. (1989). Optical constancy of the chick lens during pre- and post-hatching ocular development. *Investigative Ophthalmology and Visual Science*, 30, 967–974.
- Sroczyński, S. (1975). Die sphärische Aberration der Augenlinse des Hechts (*Esox lucius* L.). *Zoologische Jahrbücher, Physiologie*, 79, 547–558.
- Sroczyński, S. (1976). Die chromatische Aberration der Augenlinse der Regenbogenforelle (*Salmo gairdneri* Rich.). *Zoologische Jahrbücher, Physiologie*, 80, 432–450.
- Sroczyński, S. (1979). Das optische System des Auges des Flussbarsches (*Perca fluviatilis*, L.). *Zoologische Jahrbücher, Physiologie*, 83, 224–252.
- Wallman, J., Turkel, J., & Trachtman, J. (1978). Extreme myopia produced by modest change in early visual experience. *Science*, 201, 1249–1251.
- Wallman, J., Gottlieb, M. D., Rajaram, V., & Fugate-Wentzek, L. A. (1987). Local retinal regions control local eye growth and myopia. *Science*, 237, 73–76.
- Wiesel, T. N., & Raviola, E. (1977). Myopia and eye enlargement after neonatal lid fusion in monkeys. *Nature*, 266, 66–68.
- Wiesel, T. N., & Raviola, E. (1979). Increase in axial length of the macaque monkey eye after corneal opacification. *Investigative Ophthalmology and Visual Science*, 18, 1232–1236.